Phase shift induced from the dc Stark effect in an atom interferometer comprised of four copropagating laser beams

A. Morinaga and M. Nakamura
Department of Physics, Faculty of Science and Technology, Science University of Tokyo, 2641 Yamazaki, Noda-shi, Chiba 278, Japan

T. Kurosu and N. Ito
National Research Laboratory of Metrology, 1-1-4, Umezono, Tsukuba-shi, Ibaraki 305, Japan

(Received 25 May 1995; revised manuscript received 11 March 1996)

We observed the phase shift of the atomic wave function induced from the dc Stark effect using an atom interferometer comprised of four copropagating traveling laser beams. We calculated the interference signal for the interferometer in the case of a thermal atomic beam. By comparing the observed interference fringes with the calculated ones, the difference between the polarizabilities of the $^3P_1$ state and the $^1S_0$ state of calcium was obtained to be $\alpha(^3P_1)-\alpha(^1S_0)=(13.4\pm2.0)\times10^{-24}$ cm^3. This value was consistent with that deduced from the Stark frequency shift. [S1050-2947(96)51107-8]

PACS number(s): 03.75.Dg, 32.60.+i, 42.50.Vk

Atom interferometers are expected to be used as sensitive accelerometers in a variety of precision measurements such as tests of relativistic effects or quantum mechanics. In recent years, several types of the atomic interferometer have been presented and used in precision measurements [1–5]. As an application of an atomic interferometer, the electric polarizability of the ground state of sodium was measured precisely using a three-grating interferometer by Ekstrom *et al.* [6] and the difference between the polarizabilities of the excited and ground states of magnesium was measured using the Ramsey-Bordé interferometer by Sengstock *et al.* [7]. Such polarizabilities were obtained by measuring the phase shift of the atomic wave function due to the dc Stark effect, when an electric field is applied to a part of the interferometer. On the other hand, the dc Stark effect causes a shift of the resonance frequency which is generally used to obtain the difference in polarizabilities.

Recently, we developed an atom interferometer comprised of four copropagating laser beams using thermal calcium atoms [8]. In principle, the phase shift of this interferometer does not depend on laser frequency, and therefore it is less sensitive to laser frequency fluctuations than the Ramsay-Bordé atomic interferometer. The interferometer is symmetric and therefore sensitive to atomic velocity, i.e., de Broglie wavelength, in the absence of perturbation. If this interferometer is used to measure the phase shift due to the dc Stark effect, the size of interference fringes will decrease as the strength of the applied electric field increases, since the Stark phase shift depends on the atomic velocity. This is similar to the case of a white-fringe interferometer. Therefore, an accurate knowledge of the interference fringes is necessary to evaluate the phase shift. To date, only the phase relation of this interferometer has been discussed [9,10]. There has been no quantitative analysis of interference fringes in a thermal atomic beam, to our knowledge.

In this work, we use the atomic interferometer to measure the difference between the polarizabilities of the $^3P_1$ state and the $^1S_0$ state of calcium. The Stark frequency of this transition line is known to be less than 0.02 Hz/(V/cm)^2 [11]. We measure the interference fringes induced from the dc Stark effect and we analyze the Stark phase shift by comparing the experimental result with the theoretical one calculated using the evolution matrices of spinors derived by Bordé *et al.* [12]. Finally, the difference in the polarizabilities deduced from the Stark phase shift is compared with that deduced from the Stark frequency shift, which was measured independently.

The geometrical paths of an atom interacting with four laser beams are shown in Fig. 1. The atomic waves that move in the x direction interact with the laser beams that propagate in the z direction and are split into two paths: the path of the excited state b, which has a recoil velocity in the z direction in addition to the initial velocity, and the path of the ground state with an initial velocity a. After the atom interacts with the four laser beams, 16 trajectories are obtained. When the beam spacing between the first and second interaction zones is equal to that between the third and fourth ones, two Mach-Zehnder interferometers are formed by two pairs of trajectories, as seen in Fig. 1. There is little difference in physical properties between the two Mach-Zehnder

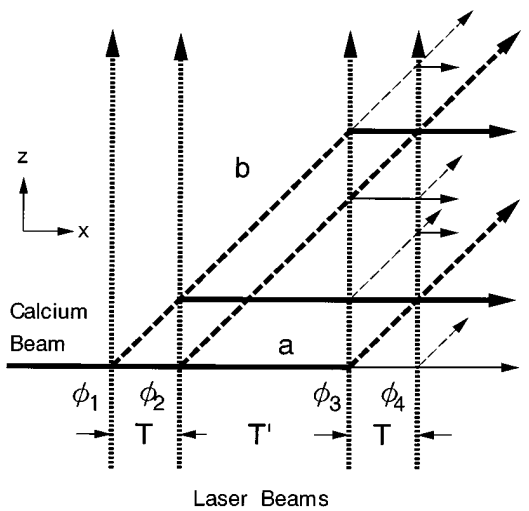

FIG. 1. Interaction geometry of the atom interferometer with four copropagating traveling laser beams. a, ground state (solid line); b, excited state (broken line); ϕ_i, phase of the ith laser beam (dotted line) at time t; and T and T' are pass times.

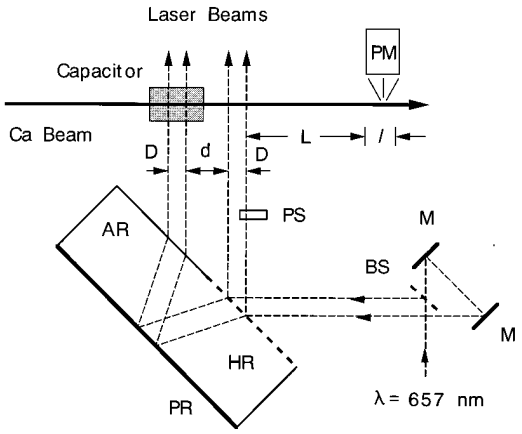

FIG. 2. Experimental setup for the calcium atom interferometer in an electric field applied by a capacitor. The four copropagating laser beams with equal power are generated by a parallel plate. AR, antireflection; HR, half reflection; and PR, perfect reflection. PM, photomultiplier; PS, phase shifter; BS, beam splitter; and M, mirror. D, d, L, and l denote length.

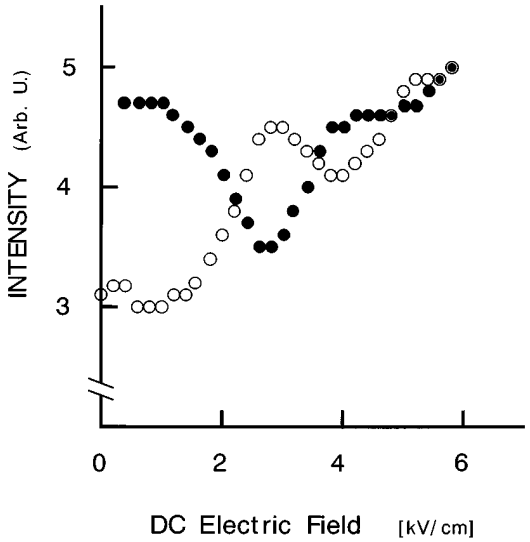

FIG. 3. Experimental result of fluorescence intensity versus dc electric field. The output power of laser beams is 0.7 mW and the distance between the first and second interaction zones is 5 mm. The oven temperature is 700 °C. Filled circle, optical phase shift of nearly π; open circle, optical phase shift of nearly zero. The error of data is equal to the point size.

interferometers, except for the state of atoms between the second and the third interaction zones.

The application of an electric field E to an atomic wave shifts the internal energy of the atoms by the Stark potential, $U(x)=-(\alpha/2)E^2$, where α is atomic polarizability. Therefore the resonance frequency between two states shifts as

$$\Delta\nu=-(\Delta\alpha/2h)E^2, \tag{1}$$

where $\Delta\alpha$ is the difference in the polarizabilities of the two states. On the other hand, an atom in the electric field changes its velocity. When the electric field is applied in the free zone between the first and second interactions in the interferometer, a phase shift occurs between the two wave functions of the atoms that are in the different states, as they have different polarizabilities. Using the Eikonal approximation, the phase shift is given by [6]

$$\Delta\varphi=\Delta\alpha DE^2/2\hbar v_x, \tag{2}$$

where D is the length of the free zone and v_x is the velocity of atoms along the x axis.

The experimental setup is shown in Fig. 2. The atom interferometer is the same as that described previously [8]. In the present experiment, a thermal calcium atomic beam was generated from an oven at a temperature of 700 °C. The most probable velocity of atoms in the flux is 780 m/s, which corresponds to a de Broglie wavelength of 13 pm. An output beam with a wavelength of 657 nm from a high-resolution dye laser spectrometer [13] was used for the excitation to the $^3P_1$ state from the ground state $^1S_0$ of Ca atoms. The beam diameter was 3.2 mm at the interaction zone. The power of each of the four laser beams was 0.7 mW. The beam spacings between the first and second interactions and between the third and fourth ones were 5 mm. The beam spacing between the second and third interactions was 15 mm. A small magnetic field was applied perpendicular to both the atomic beam and the laser beams in the interaction zone. The polarization of the laser beam was set so as to excite only the $\Delta m=0$ transition. The fluorescence from $^3P_1$ was detected at $L=250$ mm downstream by a photomultiplier with a diameter of $l=5$ cm. Under these conditions we obtained an interference signal with a visibility of 20%.

A dc electric field was applied to the first and second interaction zones using a rectangular capacitor. The capacitor has a length of 20 mm in the direction of the atomic beam and the separation between the two plates is 5 mm. The first laser beam transits at the center of the capacitor. Therefore, the strength of the electric field between the first and second interactions is uniform within an error of 3%.

The results of the fluorescence intensity versus the electric field are shown in Fig. 3. Open circles show the results when the optical phase shift $\Delta\phi$ is adjusted to nearly zero by rotating the phase shifter. Filled circles show the results when $\Delta\phi$ is nearly π. Interference fringes are observed clearly, but their size decreases as the electric field increases and the fringes disappear when the electric field is higher than 6 kV/cm. It should be noted that the number of fringes observed satisfies the uncertainty principle between spread of wave packet and momentum of atoms.

The slope of the background observed in the experimental results arises from the dc Stark frequency shift of the first and second interaction zones with the electric field from the resonance frequency of other zones without field. If the electric field is applied only to the free zone between the first and second interactions, the slope will be eliminated.

The interference fringes were calculated as follows. We consider a two-level atom interacting with four traveling laser beams that propagate in the z direction and have the same frequency ω_0. We observe the probability of atoms in the excited state by monitoring the fluorescence signal from the excited state. Therefore we consider eight trajectories, the final state of which is the excited state after interactions with the four copropagating laser beams (Fig. 1). The wave function of the atom in the excited state b is described using the evolution matrices of spinors derived by Bordé *et al.* [12].

Then the population probability of the excited state can be obtained from the product of b with its complex conjugate:

$$\begin{aligned} bb^* = & \exp(-2\gamma_b\tau)[|B_1A_2A_3A_4|^2\exp\{-\gamma_b(2T+T')\}+|D_1B_2A_3A_4|^2\exp\{-\gamma_b(T+T')\}+|B_1A_2C_3B_4|^2 \\ & \times\exp\{-\gamma_b(T+T')\}+|D_1B_2C_3B_4|^2\exp(-\gamma_bT')+|B_1C_2B_3A_4|^2\exp(-2\gamma_bT)+|D_1D_2B_3A_4|^2\exp(-\gamma_bT) \\ & +|B_1C_2D_3B_4|^2\exp(-\gamma_bT)+|D_1D_2D_3B_4|^2+\{(B_1A_2C_3B_4)(D_1B_2A_3A_4)^*\exp\{-\gamma_b(T+T')\}\exp i(\Delta\phi)+\text{c.c.}\} \\ & +\{(B_1C_2D_3B_4)(D_1D_2B_3A_4)^*\exp(-\gamma_bT)\ \exp i(\Delta\phi)+\text{c.c.}\}+O(\exp(\pm ikv_zT),\exp(\pm 2ikv_zT))], \end{aligned} \tag{3}$$

where γ_b is the relaxation constant of the excited state. τ, T, and T' are the pass times of the laser beams, the free zone between the first and second interactions, and the central free zone between the second and third interactions, respectively. A_i, B_i, C_i, and D_i are parameters related to the transition amplitude between states at the interaction zone i, as defined in Ref. [11]. $\Delta\phi=-\phi_1+\phi_2+\phi_3-\phi_4$ is an optical phase difference, where ϕ_i is the optical phase of the ith laser beam.

The first eight terms in Eq. (3) give the background population. The next two terms having the optical phase difference give the interference fringes and correspond to the two interferometers (Fig. 1). The other terms proportional to $\exp(\pm ikv_zT)$ or $\exp(\pm 2ikv_zT)$ vanish after integration over v_z on the assumption that the Doppler width is large compared to the fringe width.

The four laser beams are assumed to be Gaussian with equal power P and equal beam waist w. On resonance excitation, the parameters A_i, B_i, C_i, and D_i are given by

$$A_i=D_i=\cos[\theta(v_x)/2], \quad B_i=C_i=i\sin[\theta(v_x)/2], \tag{4}$$

and

$$\theta(v_x)=2\mu/\hbar v_x\sqrt{P/\varepsilon_0 c}, \tag{5}$$

where $\theta(v_x)$ is the pulse area and μ is the dipole moment. We measured the fluorescence signal using a photomultiplier with diameter l located at distance L from the fourth interaction zone. Finally, the fluorescence signal is averaged over the velocity distribution of atom at oven temperature T (K). Hence Eq. (3) becomes

$$\begin{aligned} bb^* = & 2\left(\frac{m}{2kT}\right)^2\int_0^\infty v_x^3\exp\left(-\frac{mv_x^2}{2kT}\right)\exp\left(-\frac{\gamma_bL}{v_x}\right)\left\{1-\exp\left(-\frac{\gamma_bl}{v_x}\right)\right\}\exp(-2\gamma_b\tau)\sin^2\left(\frac{\theta(v_x)}{2}\right)\cos^2\left(\frac{\theta(v_x)}{2}\right) \\ & \times\left\{\cos^4\left(\frac{\theta(v_x)}{2}\right)\left[1+\exp\left(-\gamma_b\frac{D}{v_x}\right)+\exp\left(-\gamma_b\frac{D+d}{v_x}\right)+\exp\left(-\gamma_b\frac{2D+d}{v_x}\right)\right]\right. \\ & +\sin^4\left(\frac{\theta(v_x)}{2}\right)\left[\exp\left(-\gamma_b\frac{D}{v_x}\right)+\exp\left(-2\gamma_b\frac{D}{v_x}\right)+\exp\left(-\gamma_b\frac{d}{v_x}\right)+\exp\left(-\gamma_b\frac{D+d}{v_x}\right)\right] \\ & \left.-2\exp\left(-\gamma_b\frac{D}{v_x}\right)\left[1+\exp\left(-\gamma_b\frac{D}{v_x}\right)\right]\sin^2\left(\frac{\theta(v_x)}{2}\right)\cos^2\left(\frac{\theta(v_x)}{2}\right)\cos\left(\Delta\phi+\frac{\Delta\alpha DE^2}{2\hbar v_x}\right)\right\}dv_x, \end{aligned} \tag{6}$$

where d is the length between the second and third interaction zones.

We calculated the interference fringes due to the dc Stark effect, using Eq. (6) under the present experimental conditions and the measured value of the dipole moment $\mu=(1.46\pm0.1)\times10^{-31}$ A s m [14]. We integrated Eq. (6) numerically over the velocity and obtained the interference fringes as a function of amplitude of the electric field multiplied by $\sqrt{\Delta\alpha}$, as shown in Fig. 4. The dotted and solid curves show the calculated fluorescence signals for the optical phase shifts $\Delta\phi=0$ and $\Delta\phi=\pi$, respectively. Except for the background slope, the calculated curves are similar to the experimental ones.

As the fringe pattern for the experimental result is distorted by the slope, we examined the difference between the signals $\Delta\phi=\pi$ and $\Delta\phi=0$. Figure 5 shows the experimental data fitted by the calculated curve, the first peak value of which is normalized to that of the experimental signal. Although the fringe height is slightly smaller than the theoretical curve, the fringe cycle is in good agreement. Hence, we deduced the difference in the polarizabilities of $^1S_0$ and $^3P_1$ $(m=0)$ states to be $\alpha(^3P_1)-\alpha(^1S_0)=(13.4\pm2.0)\times10^{-24}$ cm^3. The error was estimated roughly from the statistical error of 6% and the error of 10% due to uncertainties of the experimental values used in the calculation. For example, a decrease of D by 10% increases the value of $\Delta\alpha$ by 6%. The accuracies of dipole moment and the laser beam power, oven temperature, and so on, give errors of within a few percent.

On the other hand, the shift of the resonance frequency due to the Stark effect was measured independently to be 0.012 ± 0.002 Hz/(V/cm)^2 [15]. The frequency shift is di-

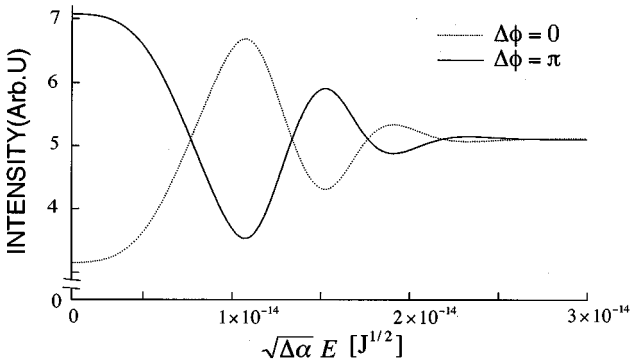

FIG. 4. Calculated result of fluorescence intensity versus dc electric field under the same condition as Fig. 3. $\Delta\phi$, optical phase shift.

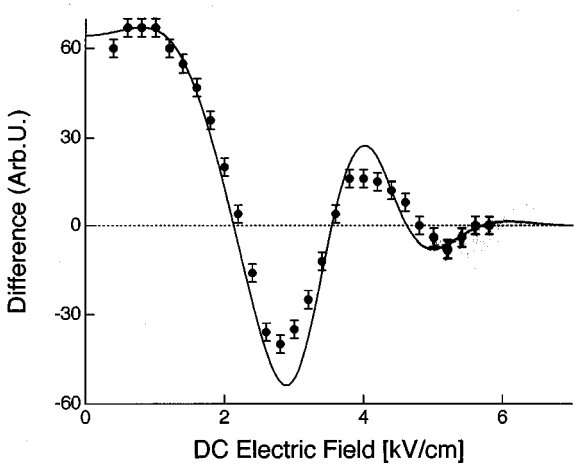

FIG. 5. Difference between signals with $\Delta\phi=\pi$ and $\Delta\phi=0$ with a calculated curve (solid line) fitted to the experimental value.

rectly converted into the difference in the polarizabilities using Eq. (1). The result is $\alpha(^3P_1)-\alpha(^1S_0)=(14.3\pm2.4)\times10^{-24}$ cm^3. The value deduced from the Stark phase shift is in good agreement with that deduced from the Stark frequency shift. This shows that the present theory is reasonably accurate.

Using the averaged value of $(13.9\pm1.7)\times10^{-24}$ cm^3 for $\Delta\alpha$ and the polarizability of the ground state $\alpha(^1S_0)=(25\pm2.5)\times10^{-24}$ cm^3, [16] we finally determined the value of the polarizability of the $^3P_1$ $(m=0)$ state to be $\alpha(^3P_1,m=0)=(39\pm3.0)\times10^{-24}$ cm^3.

In conclusion, we observed the atomic phase shift induced from the dc Stark effect using an atom interferometer comprised of four copropagating traveling laser beams. We derived a theoretical equation for the interference signal of the atom interferometer and calculated the interference fringes. The difference in the polarizabilities deduced from the Stark phase shift was consistent with that deduced from the Stark frequency shift.

Details of the calculation will be described in another paper. If we apply a dc field with the same amplitude in the reverse direction at the other two interaction zones, the phase shift due to the dc Stark shift is canceled out and the slope of the background curve is also eliminated, although the Stark frequency shift is still present. Under such conditions, a very small atomic phase shift due to the Aharonov-Casher effect should be observed [17]. For measurement of the Aharanov-Casher effect, this interferometer has the advantage of being independent of atomic velocity and frequency fluctuation of the laser. Experiments to measure the Aharanov-Casher effect are now under way.

We are grateful to J. Helmcke and K. Zeiske of Physikalisch-Technishe Bundesanstalt (Germany) for their valuable comments and suggestions concerning polarizability. We also thank Y. Ohuchi and S. Yanagimachi for their helpful contributions to this experiment and calculation.

[1] O. Carnal and J. Mlynek, Phys. Rev. Lett. **66**, 2689 (1991).
[2] D.W. Keith, Ch.R. Ekstrom, Qu.A. Turchette, and D.E. Pritchard, Phys. Rev. Lett. **66**, 2693 (1991).
[3] F. Riehle, Th. Kisters, A. Witte, J. Helmcke, and Ch.J. Bordé, Phys. Rev. Lett. **67**, 177 (1991).
[4] M. Kasevich and S. Chu, Phys. Rev. Lett. **67**, 181 (1991).
[5] F. Shimizu, K. Shimizu, and H. Takuma, Phys. Rev. A **46**, R17 (1992).
[6] C.R. Ekstrom, J. Schmiedmayer, M.S. Chapman, T.D. Hammond, and D.E. Pritchard, Phys. Rev. A **51**, 3883 (1995).
[7] K. Sengstock, U. Sterr, D. Bettermann, J.H. Muller, V. Rieger, and W. Ertmer, in *Fundamentals of Quantum Optics III*, edited by F. Ehlotzky (Springer-Verlag, Berlin, 1993), p. 36.
[8] A. Morinaga and Y. Ohuchi, Phys. Rev. A **51**, R1746 (1995).
[9] Ch.J. Bordé, in *Laser Spectroscopy*, edited by M. Ducloy *et al.* (World Scientific, Singapore, 1992), p. 239.
[10] R. Friedberg and S.R. Hartmann, Phys. Rev. A **48**, 1446 (1993).
[11] Th. Kister, K. Zeiske, F. Riehle, and J. Helmcke, Appl. Phys. B **59**, 89 (1994).
[12] Ch.J. Bordé, Ch. Salomon, S. Avrillier, A. van Lerberghe, Ch. Breant, D. Bassi, and G. Scoles, Phys. Rev. A **30**, 1836 (1984).
[13] A. Morinaga, N. Ito, and K. Sugiyama, Jpn. J. Appl. Phys. **29**, L1727 (1990).
[14] F. Riehle, A. Morinaga, J. Ishikawa, T. Kurosu, and N. Ito, Jpn. J. Appl. Phys. Lett. **31**, L1542 (1992).
[15] 12.35 ± 0.2 mHz/(V/cm)^2, K. Zeiske, G. Zinner, F. Riehle, and J. Helmcke (private communication); 12.314 ± 0.041 mHz/(V/cm)^2, J. Li and W.A. van Wijngaarden, Phys. Rev. A **53**, 604 (1996).
[16] T.M. Miller and B. Bederson, Phys. Rev. A **14**, 1572 (1976).
[17] K. Zeiske, G. Zinner, F. Riehle, and J. Helmcke, Appl. Phys. B **60**, 205 (1995).